Heliyon 10 (2024) e32499

Contents lists available at ScienceDirect

Heliyon

journal homepage: www.cell.com/heliyon

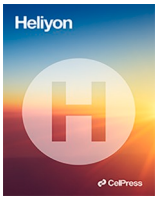

Research article

Biogenic synthesis of selenium nanoparticles from *Nyctanthes arbor-tristis* L. and evaluation of their antimicrobial, antioxidant and photocatalytic efficacy

Siddharth Satpathy [a], Lipsa Leena Panigrahi [a], Pallavi Samal [a], Kirti Kanta Sahoo [b], Manoranjan Arakha [a,*]

[a] *Centre for Biotechnology, Siksha 'O' Anusandhan (Deemed to Be University), Bhubaneswar, 751003, Odisha, India*
[b] *School of Civil Engineering, Kalinga Institute of Industrial Technology Univ., Bhubaneswar, Odisha, 751024, India*

ARTICLE INFO

Keywords:
Selenium nanoparticles
Photocatalytic activity
Antimicrobial activity
Dye degradation
Membrane damage

ABSTRACT

Biogenic synthesis of nanoparticles has been established as an environmentally benign and sustainable approach. This study emphasizes biosynthesis of selenium nanoparticles (SeNPs) utilizing leaf extract of *Nyctanthes arbor-tritis* L., well known for its abundant bioactive compounds. Various analytical techniques were employed for characterization of synthesized SeNPs. X-ray diffraction (XRD) spectroscopy confirmed the crystalline structure and revealed the average crystalline size of SeNPs to be 44.57 nm. Additionally, UV–Vis spectroscopy confirmed successful synthesis of SeNPs by validating the surface plasmon resonance (SPR) properties of SeNPs. FTIR analysis data revealed different bonds and their corresponding functional groups responsible for the synthesis and stability of synthesized SeNPs. DLS and zeta analysis revealed that 116.5 nm sized SeNPs were stable in nature. Furthermore, field emission scanning electron microscopy (FE-SEM) validated the spherical morphology of SeNPs with a size range of 60–80 nm. Inductively coupled plasma-optical emission spectroscopy (ICP-OES) determined the concentration of SeNPs in the obtained colloidal solution. Antioxidant activity of synthesized SeNPs was evaluated employing DPPH and H_2O_2 assay, revealed that the synthesized SeNPs were effective antioxidant agent. Additionally, antimicrobial potential was evaluated against a panel of Gram-positive and Gram-negative bacteria and found to be effective at higher concentration of SeNPs. SeNPs also exhibited strong anti-biofilm activity while evaluated against various biofilm producing bacteria like *Escherichia coli, Staphylococcus epidermidis* and *Klebsiella pneumonia*. The cytotoxicity of the bio-synthesized SeNPs was evaluated against HEK 293 cell line, exhibited minimal toxicity even at concentration 100 μg/mL with 65% viable cells. SeNPs has also been evaluated for dye degradation which has indicated excellent photocatalytic activity of synthesized SeNPs. The experimental data obtained altogether demonstrated that synthesized SeNPs exhibited significant antimicrobial and anti-biofilm activity against various pathogens, and also showed significant antioxidant and photocatalytic efficiency.

* Corresponding author. Centre for Biotechnology, Siksha 'O' Anusandhan (Deemed to be University), Bhubaneswar, India.
E-mail addresses: manoranjan.arakha@gmail.com, marakha@soa.ac.in (M. Arakha).

https://doi.org/10.1016/j.heliyon.2024.e32499
Received 17 December 2023; Received in revised form 26 May 2024; Accepted 5 June 2024
Available online 8 June 2024

Abbreviations

N. arbor-tristis L.	*Nyctanthes arbor-tristis* Linn
SeNPs	Selenium Nanoparticles
XRD	X-ray diffraction
UV	Vis- Ultraviolet–Visible
SPR	Surface Plasmon Resonance
FTIR	Fourier Transform Infrared Spectroscopy
FE-SEM	Field Emission Scanning Electron Microscopy
DLS	Dynamic Light Scattering
ICP-OES	Inductively Coupled Plasma-Optical Emission Spectroscopy
O.D-	Optical density
AMR	Antimicrobial resistance
CDC	Centers for Disease Control and Prevention
MDR	Multidrug resistance
ROS	Reactive Oxygen Species
IMTECH	Institute of Microbial Technology
DPPH	2,2-diphenyl-1-picrylhydrazyl
BHIB	Brain heart infusion broth
CRA	Congo-red agar
MB	Methylene blue

1. Introduction

The inevitable genetic evolution of bacteria to resist antibiotics has reached peak levels in the twenty-first century, making antimicrobial resistance (AMR) a severe health concern that could have global effects and appeals for immediate action [1]. Not only in developing countries rather AMR has been recognized as a serious risk to public health systems globally. For instance, it has been estimated that antibiotic resistance costs more than nine billion euros in Europe annually [2]. However, according to the Centres for Disease Control and Prevention (CDC), antibiotic resistance increases healthcare expenditures in the USA by 20 billion dollars annually [3]. According to the recent evolving scenario of scientific research, nanotechnology has established remarkable and innovative perceptions towards divergent and efficient applications in the health sector to environmental remediation [4]. Nanotechnology has also established its potential in combatting AMR strains [5]. Due to their distinctive physicochemical characteristics, nanoparticles are capable of encountering antibiotic resistance mechanisms by employing a variety of novel bactericidal pathways to generate antimicrobial action [6]. Additionally, nanomaterials may bind to and rupture bacterial membranes, resulting in leakage of cytoplasmic components [7,8]. Membrane disruption induces oxidative stress, enzyme inhibition, and electrolyte imbalance which ultimately lead to cell death. In this regard, Rai et al. have demonstrated that silver nanoparticles have the potential to be an alternative for antibiotics while dealing with microbial infections prompted by multidrug resistance (MDR) pathogens [9]. Some metal oxide nanoparticles, including ZnO and TiO_2, have been reported to have the potential to kill bacteria by generating reactive oxygen species (ROS), while others have the propensity to damage cell membranes due to their physicochemical properties and metal ion release [10,11].

Current scientific findings have estimated the effectiveness of green synthesis methodology for obtaining stable, safe, eco-friendly and cost-effective nanoparticles [12]. Additionally, nanoparticles formulated adopting the green synthesis methods are found to be less toxic and biocompatible in nature [13]. Furthermore, functional groups of phytochemicals like amines and alkanes are essential for the synthesis of nanoparticles which are generally native to various plant-based metabolites resulting in the reduction of metal ions into nanoparticles [14].

Selenium, being a vital trace mineral has a significant role in maintaining human health [15,16]. According to the recent scientific approach, SeNPs are gaining significant attention due to their low toxicity, biocompatibility, high specific surface area, high catalytic efficiency and adsorption ability [17]. Recent research progress on SeNPs has put its significance over various grounds. In this context, Khurana et al. have estimated the efficiency of SeNPs in pharmacological applications along with mitigating various inflammatory and oxidative stress-mediated disorders [18]. Probiotics or non-pathogenic organisms derived SeNPs can be beneficial in combatting cancer as well as considered to be less harmful to the human body as stated by Ullah et al. [19]. According to Bao et al. SeNPs are also

Table 1
Parameters set for ICP-OES measurement.

Condition Set 1			
Read time (s):	5	Nebulizer flow (L/min):	0.7
RF power (kW):	1.2	Plasma flow (L/min):	12
Stabilization time (s):	60	Aux flow (L/min):	1
Viewing mode:	Axial	Make up flow (L/min):	0
Viewing height (mm):	N/A	Oxygen %:	0

reliable candidates for agricultural applications since they can help in alleviating numerous biological and abiotic stresses like salinity, heavy metals, drought and high temperature and also can be helpful in the inhibition of pathogenic microorganisms in crops [20]. Literature states that SeNPs are very effective as fertilizer for the improvement of crop yield [21]. SeNPs have also put their significance in the elimination of free radicals for the protection of crops from oxidative damage [22]. SeNPs can be useful in the improvement of yield and quality of agricultural products along with human health [23]. Previously, biosynthesis of SeNPs has been reported from various bacteria, fungi as well as various plant extracts [24]. Generally, plant extracts serve as an effective reducing agent for the synthesis of SeNPs as they are rich in protein, amino acids, vitamins etc [23]. On account of biosynthesis of SeNPs, Hashem et al. have proposed the synthesis of SeNPs from aqueous extract of nettle leaves and evaluated their antibacterial activity against various bacterial strains. Here, SeNPs showed excellent antibacterial activity [25]. Additionally, Pandey et al. have demonstrated successful biosynthesis of SeNPs from cyanobacteria and investigated relevant applications like antibacterial, anti-biofilm, antioxidant and photocatalytic degradation, thereby proving the versatility of SeNPs in various biomedical fields [26]. Similarly, Saied et al. have demonstrated the biosynthesis of SeNPs from *Aspergillus terreus* and proved significant antimicrobial and photocatalytic activities of SeNPs [27]. Additionally, biosynthesized SeNPs from *Eleagnus indica* leaf extract have showed effective antimicrobial activity and photocatalytic activity as suggested by Indhira et al. [28].

N. arbor-tristis L. generally considered as night flowering jasmine or harsingar, belongs to the family Oleaceae, also well-known as the "tree of sorrow" since it shines at dusk and loses its brightness at dawn. Generally, these are shrubs with a height of 10 m and broad leaves. The flowers possess a pleasant aroma with five to eight-lobed white corolla with an orange-red centre, generally found in clusters. *N. arbor-tristis* L. plants are generally native to southern Asia and have been widely distributed across various regions from northern Pakistan and southern Nepal to northern India and southeast Thailand [29]. *N. arbor-tristis* L. has been widely recognized in traditional medicine owing to its significant pharmaceutical applications as anti-allergic, antihistaminic, purgative, antibacterial, antiviral, anti-fungal, anti-helminthic, anti-amoebic, anti-oxidant, anti-cancer, anti-diabetic, immunomodulatory, CNS modulatory, hepatoprotection, diuretic, wound healing and ulcerogenic agent [29–31]. Hence, such multidisciplinary actions of *N. arbor-tristis* L. make it a reliable candidate for the synthesis of eco-friendly, cost-effective, less toxic, biocompatible, stable, and safe nanoparticles.

In our study, we have focussed on the synthesis of SeNPs using leaf extract of *N. arbor-tristis* L., since it contains phytochemicals such as mannitol, vitamin C, carotene, flavanol glycosides, triterpenoid, β-sitosterol etc. which will act as both reducing and capping agent in the fabrication of SeNPs [29,32]. Moreover, our study offers comprehensive insight regarding eco-friendly SeNPs synthesis in addition to an evaluation of their antimicrobial, anti-biofilm, antioxidant, and photocatalytic activity. We have also investigated the effect of SeNPs on cytoplasmic membrane integrity as it is an essential aspect of their antibacterial mechanism. The significance of our study ultimately relies upon the possibility of delivering eco-friendly approaches for nanoparticle synthesis to promote green nanotechnology, paving the way to innovative applications in the domains of health care and ecological management.

2. Materials and methods

Acenetobacter baumannii (MTCC 1245), *Micrococcus luteus* (MTCC 106) *Escherichia coli* (MTCC 443), *Klebsiella Pneumonia* (MTCC 109), *Staphylococcus epidermidis* (MTCC 435) were obtained from Institute of Microbial Technology (IMTECH), Chandigarh, India. brain heart infusion broth (BHIB), nutrient agar, nutrient broth, Congo red, 2,2-diphenyl-1-picrylhydrazyl (DPPH) and ascorbic acid (Vitamin C) were purchased from SRL Pvt. Ltd, Mumbai, India. Hydrogen peroxide (H_2O_2) was purchased from Molychem Pvt. Ltd, Mumbai, India. Sodium selenate anhydrous was obtained from HiMedia Laboratories Pvt. Ltd, India. The chemicals used for the entire work were of analytical grade and utilised without additional purification.

2.1. Synthesis of selenium nanoparticles

For the synthesis of SeNPs, *N. arbor-tristis* L. plant samples were collected from the locality of Bhubaneswar, Odisha, India. The leaves were collected and washed with tap water thoroughly. Subsequently, they were sun-dried for a week. The leaves were ground using a mechanical grinder. 1 gm of the powdered leaves were dissolved in 100 mL of distilled water and kept at stirring for 15 min followed by heating at 60^{o}C for 30 min. The solution was centrifuged at 10,000 rpm for 15 min. After that, the supernatant was collected and filtered using a Whatman's filter paper. To the plant extract, 50 mL of 0.1 M sodium selenate salt was added. Then the reaction mixture was kept for incubation at 37^{o}C and 120 rpm agitation for 24 hr. After 24 hr of incubation, the colour change was noticed, which showed the synthesis of SeNPs. The obtained SeNPs solution was further purified by centrifugation at 10,000 rpm for 20 min and the obtained supernatant was dried at 80^{o}C.

2.2. Characterization of biosynthesized SeNPs

The absorbance of biosynthesized SeNPs and *N. arbor-tristis* L. leaf extract was analysed using UV–Vis spectroscopy (HITACHI, Tokyo, Japan). Bond level characteristics were obtained using an FTIR spectroscope (JASCO, Japan). The hydrodynamic size of colloidal SeNPs was measured by DLS (Malvern Panalytical Ltd.). The surface potential of the colloidal SeNPs was measured by a zeta sizer (Malvern Panalytical). XRD pattern of synthesized SeNPs was documented using smart lab version Rigaku X-ray Diffractometer (Tokyo, Japan), applying Cu-Kα radiation, at a scan rate of 20^{o}/min having a 2θ range of 20^{o} to 80^{o}. Distinctive phases available in the synthesized SeNPs sample were analysed by the X′-pert high score software owning search and match facility. Morphological characteristics of biosynthesized SeNPs were studied by FE-SEM (JEOL JSM-IT800). The concentration of the synthesized SeNPs in the colloidal solution was measured by ICP-OES (Agilent ICP-OES 5100).

2.3. Evaluation of antioxidant activity of biosynthesized SeNPs

2.3.1. Evaluation of free radical scavenging activity by DPPH assay

The antioxidant activity of synthesized selenium nanoparticles was assessed by DPPH (2,2-diphenyl-1-picrylhydrazyl) free radical scavenging assay. Precisely, a methanolic stock solution of 0.2 mM DPPH was prepared. Here ascorbic acid (Vitamin C) was taken as a standard. In a 96 well microtiter plate, 100 μL aqueous solution of different concentrations of selenium nanoparticles (10, 20, 50, 100, 250 μg/mL) was added with 100 μL of DPPH methanolic solution. Later on, the reaction mixtures were undergone incubation in dark environment with a constant shaking at an optimum temperature of 35°C for 30 min. The absorbance of DPPH radical scavenging activity was noted using a spectrophotometer at 517 nm through a Biorad imark microplate reader. Afterward, the free radical scavenging activity was estimated by applying the formula.

$$\text{Radical scavenging activity } (\%) = \left(A_{control} - A_{sample} \ / \ A_{control}\right) \text{ x } 100$$

The result was obtained following a plot between % DPPH free radical scavenging against the concentration of SeNPs along with the control (μg/ml).

2.3.2. Hydrogen peroxide scavenging assay

Initially, 40 mM of H_2O_2 solution was prepared in phosphate buffer solution. Ascorbic acid (Vitamin C) was considered as a positive control. 2 mg/mL SeNPs stock solution was also prepared in phosphate buffer. 1 mL of SeNPs of various concentrations (10, 20, 50, 100, 250, 500 μg/mL) was added with 1 mL of H_2O_2. After 10 min, the absorbance was determined at 230 nm. Subsequently, the percentage of inhibition was determined applying the following formula.

The results were interpreted by plotting a graph between % of H_2O_2 free radical scavenging and the concentration of SeNPs.

2.4. Evaluation of antimicrobial activity of biosynthesized SeNPs

2.4.1. Growth kinetics assay

The antimicrobial activity of biosynthesized SeNPs was determined against Gram-negative bacteria like *A. baumannii*, *E. coli,* and Gram-positive bacteria like *M. luteus* with the help of a growth kinetics study. Precisely, a loop containing bacterial culture was collected from the mother culture inoculated into the nutrient broth and kept for overnight incubation at 37°C and 120 rpm in a shaker incubator. Furthermore, by dissolving appropriate quantity of SeNPs in distilled water and after 20 min of sonication, a stock solution of biogenic SeNPs was prepared. 96 well plate containing different concentrations of SeNPs (10, 25, 50, 100, 250, 500 μg/mL) was employed for the preparation of the reaction mixtures of growth kinetics study, while reaction mixtures devoid of SeNPs was considered as control. 20 μL of bacterial culture was added to each reaction mixtures and by adding appropriate quantity of nutrient broth the volume was fixed up to 300 μL. A plate reader (Biorad imark plate reader) was used to assess the growth kinetic study by estimating the optical density (O.D) at 600 nm.

2.4.2. Analysis of cytoplasmic leakage

Primarily, *S. Epidermidis* and *E. coli* were cultured and were kept under overnight incubation for the evaluation of leakage of cytoplasmic materials such as nucleic acids and proteins. Post incubation, the microbial culture was centrifuged at 10,000 rpm for 10 min. Then the pellet was suspended in PBS buffer (PBS 7.4). The bacterial cell count was set to 10^5 cells/mL. Cell suspensions were further added with SeNPs followed by incubation at room temperature for 2, 4, and 6 hr. The bacterial culture devoid of nanoparticles was taken as a control. Thereafter, the cultures were purified via centrifugation at 5000 rpm for 10 min and subsequently, the absorbance of obtained supernatants was measured at 260 nm and 280 nm to estimate leakage of nucleic acids and proteins respectively.

2.4.3. Anti-biofilm activity

The effect of biogenic SeNPs on bacterial biofilm formation was evaluated by the 96-well plate method. Precisely, bacterial culture of *E. coli, S. epidermidis* and *K. pneumonia* was cultured in nutrient broth following overnight incubation at 37°C. A 96-well plate containing different concentrations of SeNPs (25, 50, 100, 250, 500 μg/mL) was employed for preparation of the reaction mixtures for bacterial biofilm inhibition study. Afterward, 20 μL of bacterial culture was added to each reaction mixture of the plate for further study. Reaction mixtures which were not subjected to SeNPs treatment were considered as control. Following, the microtiter plate underwent incubation for 48 hr at 37°C. Post incubation, the wells were further washed with phosphate buffer (PBS 7.4) followed by treatment with 200 μL of 0.1% crystal violet solution. Afterward, the plate was incubated for 1 hr and then crystal violet solution was removed. The unbounded cells were removed via washing the wells with phosphate buffer saline for 10 min. The biofilm was dissolved by mixing 200 μL of 95% ethanol and later on, the plates were dried. A Biorad imark plate reader was used to measure the OD of each well at 600 nm.

2.4.4. Congo-red plate assay

By using Congo-red plate assay, anti-biofilm activity of biosynthesized SeNPs was further evaluated. Precisely, the biofilm forming capacity of *K. Pneumonia* and *S. epidermidis* bacterial strain was carried out on Congo red agar (CRA) plate. The media was prepared using Congo red, agar, sucrose, brain heart infusion (BHI) broth and distilled water following the method proposed by Sahoo et al.

[33]. Various concentrations of SeNPs (100, 250 and 500 μg/mL) was prepared and sonicated for further use. Afterward, different concentrations of prepared SeNPs were mixed with the media. The media containing SeNPs was poured into individual plates and solidified. The *K. Pneumonia* and *S. epidermidis* bacterial strains were streaked on the plates with various concentrations of SeNPs and it was kept for 48 hr incubation at 37°C to estimate the effectiveness of SeNPs on inhibition of biofilm.

2.5. Evaluation of photocatalytic activity of biosynthesized SeNPs

The photocatalytic activity of biosynthesized SeNPs synthesized from *N. arbor-tristis* L. was evaluated by degradation of a cationic dye like methylene blue (MB). 10 ppm of dye was dissolved in 300 mL of distilled water to prepare the stock solution of MB dye. 2 mg/mL SeNPs stock solution was prepared in distilled water and this solution was sonicated for 20 min. Both SeNPs solution and MB dye were added in an equal ratio. The reaction mixture was sonicated for 20 min. After 20 min of sonication the reaction mixture was undergone stirring at 600 rpm for 20 min. MB dye solution devoid of SeNPs was considered as control. Subsequently, the solution was kept in UV after addition of 5 mL of H_2O_2. The reactions were observed through a UV–Vis spectroscopy, monitoring the absorbance in the range of 200–800 nm at a regular time of 10 min.

2.6. Cytotoxicity assay of biosynthesized SeNPs

The cytotoxicity of biosynthesized SeNPs was assessed against the human embryonic kidney (HEK 293, NCCS Pune, India) cell line with the help of Alamar Blue dye reduction assay, following the protocol proposed by Arakha et al. [34]. Briefly, 5000 HEK 293 cells were seeded in each well of a 96-well plate with Dulbecco's Modified Eagle's Medium (DMEM, Himedia, India), containing 10% fetal bovine serum (FBS). The culture medium was undergone incubation for 24 hr in a CO_2 incubator. Post incubation, the culture medium was added with fresh DMEM medium having different concentrations of SeNPs (5, 10, 25, 50, 100 μg/mL). The bio-synthesized SeNPs were freshly prepared before the assay by dispersing 2 mg/mL of SeNPs in phosphate buffer (PBS 7.4) and sonicated for 20 min. After the addition of the SeNPs, the cells were kept under incubation for the next 24 hr. Before the collection of samples, each well was added with 10% v/v Alamar Blue dye (Invitrogen, USA) and was kept under incubation for 2 hr. Then the fluorescence intensity was measured at 590 nm with an excitation wavelength at 544 nm. The percentage of viable cells in the untreated (control) and SeNPs treated samples were quantified with the help of the recorded ratio of fluorescence intensity in treated to untreated cells.

2.7. Statistical analysis

All the experiments were done in triplicates and the results were assessed as mean ± SD. The data analysis was done with one-way ANOVA using Minitab software. The statistical analysis was done with Tukey's multiple comparison test. $P \leq 0.05$ were considered significant.

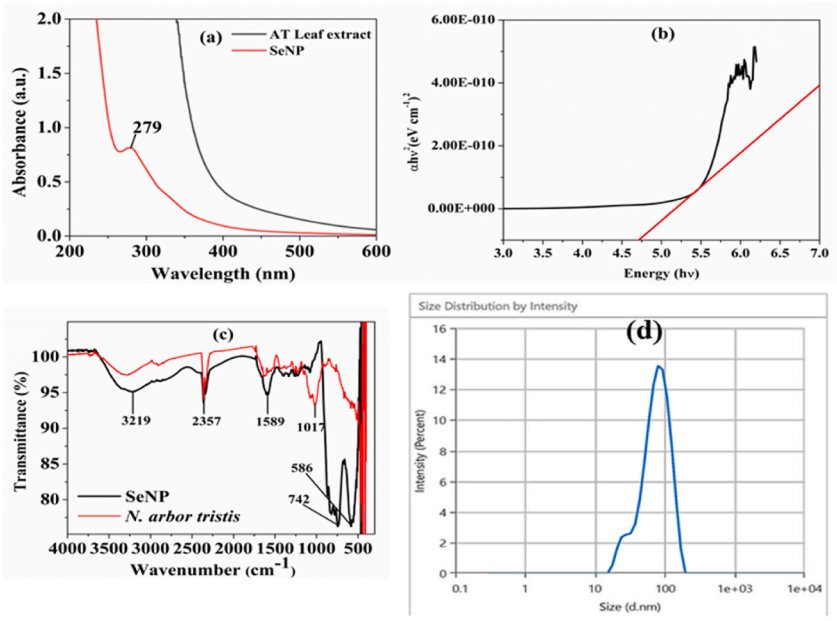

Fig. 1. Characterization of biogenic SeNPs: (a) Absorption spectra analysis using UV–Vis spectroscopy (b) Band gap energy analysis through Tauc plot, (c) Bond level characterization using Fourier Transform Infrared Spectroscopy, (d) Hydrodynamic size analysis of biosynthesized SeNPs.

3. Results

3.1. Characterization of biosynthesized SeNPs

3.1.1. UV–Vis characterization

Upon analysis in a range of 200–800 nm using UV–Vis spectroscopy, owing to the surface plasmon resonance (SPR) characterization resulting from the presence of conduction electrons on the surface of SeNPs, the synthesized SeNPs revealed a significant absorption peak at 279 nm (Fig. 1a) [35]. Additionally, we did not observe any prominent peak for the leaf extract in the studied wavelength range. Subsequently, Cittrarasu et al. have also observed absorption peak at 277.5 nm. Additionally, Mellinas et al. have also obtained the peak at 276 nm [36,37]. The band gap energy of synthesized SeNPs was calculated to be around 4.68 eV (Fig. 1b) using the following equation.

$(\alpha h\nu)^n = A(h\nu - E_g)$ [37].

Where E_g represents energy band gap, α relates to optical absorption coefficient, h signifies Plank's constant, ν is the frequency of light, A is known as constant of proportionality and n = 2 which denotes direct band gap energy [37].

3.1.2. Bond level characterization of SeNPs

FTIR analysis confirmed various bonds present in green synthesized SeNPs and the plant extract (Fig. 1c). As shown in figure, absorption peak obtained around 3219 cm^{-1} in SeNPs is due to the occurrence of O–H bond possessed by alcohol and phenols [38]. Similarly, the absorption peak achieved at 2357 cm^{-1} for both plant extract and SeNPs can be assigned as the peak of CO_2 [38]. Additionally, we have also observed other significant peaks obtained at 1589 cm^{-1} confirming presence of N–O bond corresponding to nitro compounds. Subsequent absorption peak achieved at 1017 cm^{-1} confirms the existence of C–N bond which possesses aliphatic amines. The absorption spectra of SeNPs shows prominent peaks at 742 cm^{-1} and 586 cm^{-1} which signifies Se–Se/Se–O bond

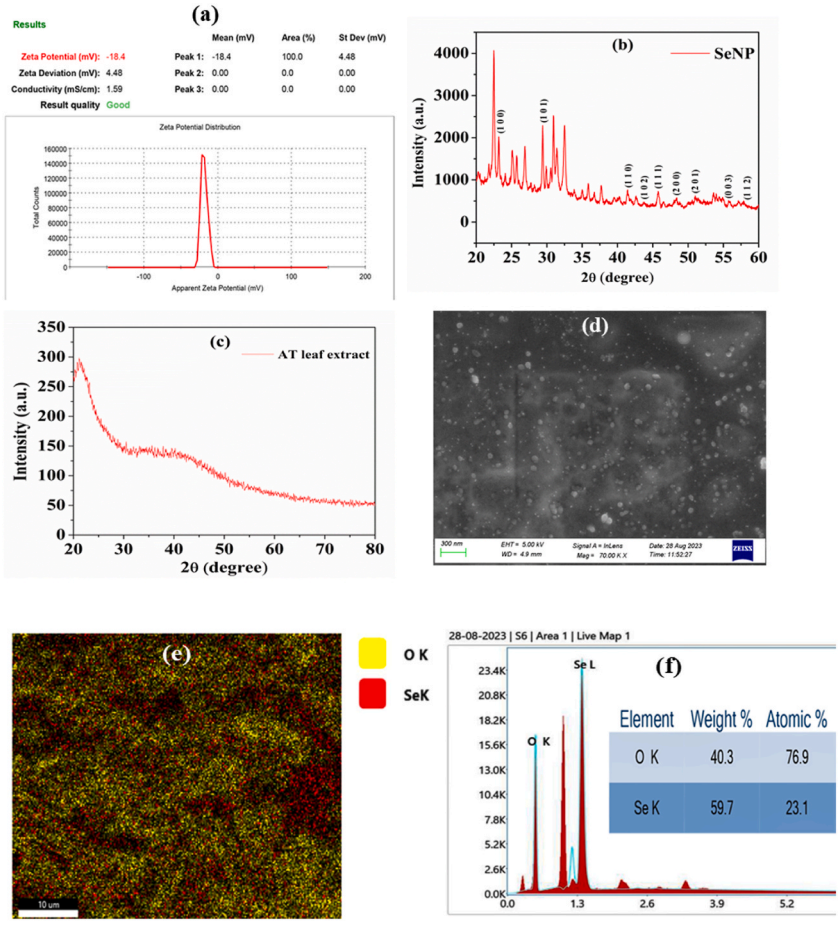

Fig. 2. (a) Zeta potential of the biosynthesized SeNPs, (b) X-ray diffraction analysis of SeNPs and (c) X-ray diffraction analysis of plant extracts (d) Morphological analysis of biosynthesized SeNPs by FE-SEM, (e) and (f) Elemental analysis by EDAX.

vibrations confirming the biosynthesis of SeNPs [39].

3.1.3. Hydrodynamic size analysis of biosynthesized SeNPs

The hydrodynamic size of synthesized SeNPs was determined by DLS (Fig. 1d). The hydrodynamic diameter (d.nm) was obtained in the x-axis and scattering intensity was represented in the y-axis. From the plotted graph, the average size of the synthesized SeNPs was obtained at 116.5 nm and the PDI (polydispersity index) value was about 0.4026 nm.

3.1.4. Zeta potential analysis of biosynthesized SeNPs

Zeta potential analysis was estimated to investigate the stability of nanoparticles in a colloidal solution. The biosynthesized SeNPs revealed a zeta potential value of about −18.4 mV (Fig. 2a). The magnitude of zeta potential indicated that the synthesized SeNPs were relatively negatively charged in nature. Subsequently, the biosynthesized SeNPs were stable in colloidal solution to a certain extent.

3.1.5. X-ray diffraction analysis of SeNPs

The XRD pattern confirmed the crystalline structure of synthesized SeNPs with peaks at characteristic diffraction 2θ angle values of 23.51^0, 29.70^0, 41.30^0, 43.64^0, 45.35^0, 48.10^0, 51.72^0, 55.66^0 and 56.14^0 resulting with significant indices (100), (101), (110), (102), (111), (200), (201), (003) and (112) respectively (Fig. 2b). Such indices have further revealed the hexagonal structure of SeNPs [40, 41] according to JCPDS (Joint Committee on Powder Diffraction Standards) reference code 06–0362. Our work is in good agreement with Srivastava et al. [42]. Additionally, we have also estimated the average crystalline size of selenium nanoparticles applying Scherrer's equation: $D = K\lambda/\beta\cos\theta$. Where λ is the wavelength of X-ray, K is shape factor or proportionality coefficient, θ indicates Bragg angle and β referred to as full width at half maximum in radians. The average size of the synthesized SeNPs was found to be 44.57 nm. Additionally, the *N. arbor-tristis* L. leaves powder was also analysed by XRD (Fig. 2c). The XRD analysis of leaves powder was found to be amorphous in nature. The lack of any significant peak is attributed to the organic groups present in the leaves.

3.1.6. Morphological characterization of SeNPs

FE-SEM analysis revealed the morphological characteristics of synthesized SeNPs. The biosynthesized SeNPs were found to be spherical and within the size range of 60–80 nm (Fig. 2d). Energy-dispersive X-ray spectroscopy has further confirmed the synthesis of SeNPs providing information regarding the elemental composition of the particles with 59.7 % of selenium element being present (Fig. 2e and f).

3.1.7. ICP-OES measurements

The basic principle underlying the instruments involves the determination of signal intensity formed after ionization of each particle rather than the constant flow of ions reaching the plasma. Our results determined the SeNPs concentration as 1269 ppm (Table 1).

4. Antioxidant activity of SeNPs

4.1. Evaluation of free radical scavenging activity of biosynthesized SeNPs by DPPH assay

DPPH is well known as a stable organic compound commonly used to measure free radical scavenging activity, which has nitrogen radicals at the center and exhibits a deep purple color. In this assay, the antioxidant compound generally interacts with DPPH by donating electrons or hydrogen atoms to neutralize the free radical appearance of DPPH. We have investigated the antioxidant activity

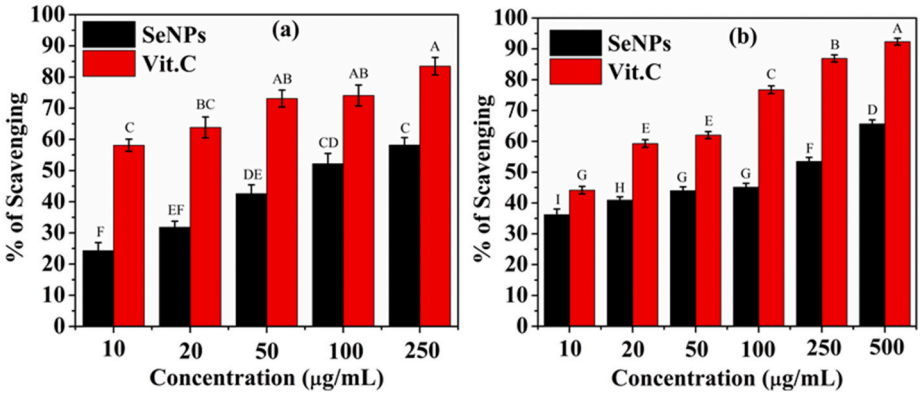

Fig. 3. Comparative analysis of radical scavenging activity of biogenic SeNPs and Vitamin C via (a) DPPH assay and (b) H_2O_2 scavenging activity. These experiments were carried out independently in triplicates and data were stated as mean ± SD. Tukey's multiple comparison test was used to evaluate the level of statistical significance amongst the test samples considering $p \leq 0.05$ as significant. The bar graphs indicating single alphabetic letters in the corresponding study were significant. Means that do not share a letter are significantly different.

of synthesized SeNPs using a DPPH assay taking ascorbic acid as control (Fig. 3a). Ascorbic acid undoubtedly showed effective scavenging activity even at lower concentrations, but SeNPs showed more than 50% of scavenging activity at 100 μg/mL and 250 μg/mL. This concluded that, at higher concentrations, SeNPs show significant antioxidant activity.

4.2. Hydrogen peroxide scavenging activity of biosynthesized SeNPs

Antioxidant activity of synthesized SeNPs was further estimated by H_2O_2 radical scavenging assay taking ascorbic acid as a control. Even at low concentrations, ascorbic acid showed significant scavenging activity, whereas at 50 and 100 μg/mL, SeNPs did not show significant scavenging activity (Fig. 3b). On the other hand, at higher concentrations of SeNPs such as 250 μg/mL, SeNPs showed up to 52% and at 500 μg/mL it showed up to 65% of radical scavenging activity. Interestingly, at higher concentrations (500 μg/mL) both SeNPs and ascorbic acid have exhibited maximum scavenging activity (Fig. 3b). Lobo et al. suggested that antioxidants are compounds that can neutralize or mitigate the damaging effects of free radicals, such as H_2O_2 radicals [43]. For comparison, ascorbic acid, formerly known as vitamin C, was used as a reference or standard antioxidant. The study aimed to compare the antioxidant potential of ascorbic acid and SeNPs at various concentrations. This study estimated that ascorbic acid showed higher antioxidant activity even at low concentrations, while SeNPs demonstrated significant scavenging activity at 250 and 500 μg/mL.

5. Antimicrobial activity of synthesized SeNPs

Growth kinetics studies were carried out to analyse the antimicrobial activity of the biosynthesized SeNPs against Gram-negative bacteria like *A. baumannii*, *E. coli* and Gram-positive bacteria like *M. luteus* at various concentrations of SeNPs (10, 25, 50, 100, 250, 500 μg/mL) (Fig. 4). Here, lower concentrations of SeNPs showed negligible inhibition of bacterial growth. However, as the concentration of SeNPs reached up to 250 and 500 μg/mL, growth inhibition was significantly observed against Gram-negative bacteria like *A. baumannii* (Fig. 4a), *E. coli* (Fig. 4b) and Gram-positive bacteria like *M. luteus* (Fig. 4c) respectively in comparison to control. The acquired growth kinetics data for different concentrations of SeNPs exhibited the reduction of cell viability in accordance with an increase in the concentration of SeNPs. In this framework, San Keskin et al., Salem et al. have also observed significant antimicrobial activity of SeNPs [44,45]. Additionally, in our study significant growth inhibition was evidenced at higher concentration of SeNPs against *A. baumannii*, *E. coli* and *M. luteus*.

5.1. Analysis of cytoplasmic leakage

Nanoparticles can be successful in triggering cytoplasmic leakage across the bacterial cell membrane, by rupturing the cellular membrane [46]. To acquire an improved grasp of the influence of SeNPs on bacterial membranes, we have estimated the leakage of cytoplasmic components like nucleic acids and proteins of *E. coli* and *S. epidermidis* upon treatment with SeNPs. The findings from our study demonstrated significant increase in the absorbance of bacterial culture with an increase in time i.e. from 2 hr, to 6 hr. Reasonably, upon treatment with increasing concentrations of SeNPs, we have noticed a remarkable increase in the absorbance of *E. coli* bacterial culture in contrast to the control (Fig. 5a). Additionally, we have also observed similar results in the case of *S. epidermidis* upon treatment with a similar concentration of SeNPs, demonstrating cytoplasmic leakage of nucleic acid content of test bacteria upon treatment with SeNPs (Fig. 5b). However, we have also estimated the amount of cytoplasmic leakage content such as protein upon treatment with SeNPs by observing optical density of bacterial culture at 280 nm. As shown in Fig. 5c and d, upon treatment with different concentrations of SeNPs, we have observed increasing optical density of bacterial culture at 280 nm demonstrating leakage of cytoplasmic protein in both the test bacteria *E. coli* (Fig. 5c) and *S. epidermidis* (Fig. 5d).

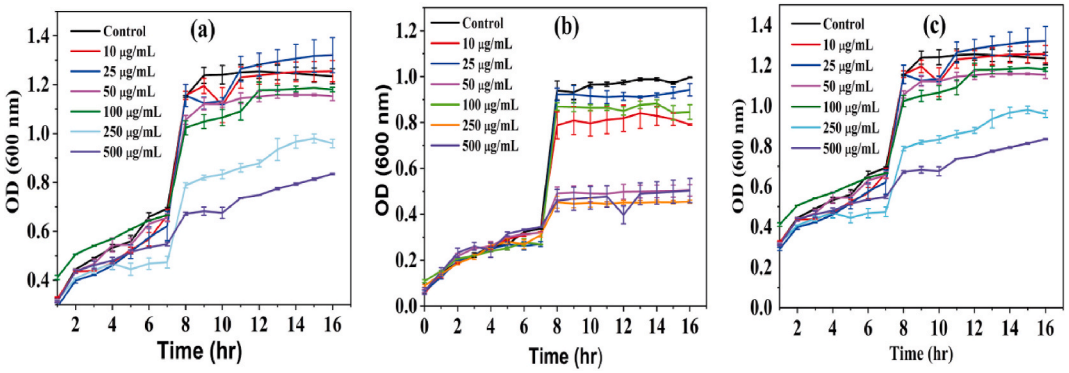

Fig. 4. Growth kinetic analysis of (a) *A. baumannii*, (b) *E. coli*, (c) *M. luteus* in presence of different concentration of biogenic SeNPs.

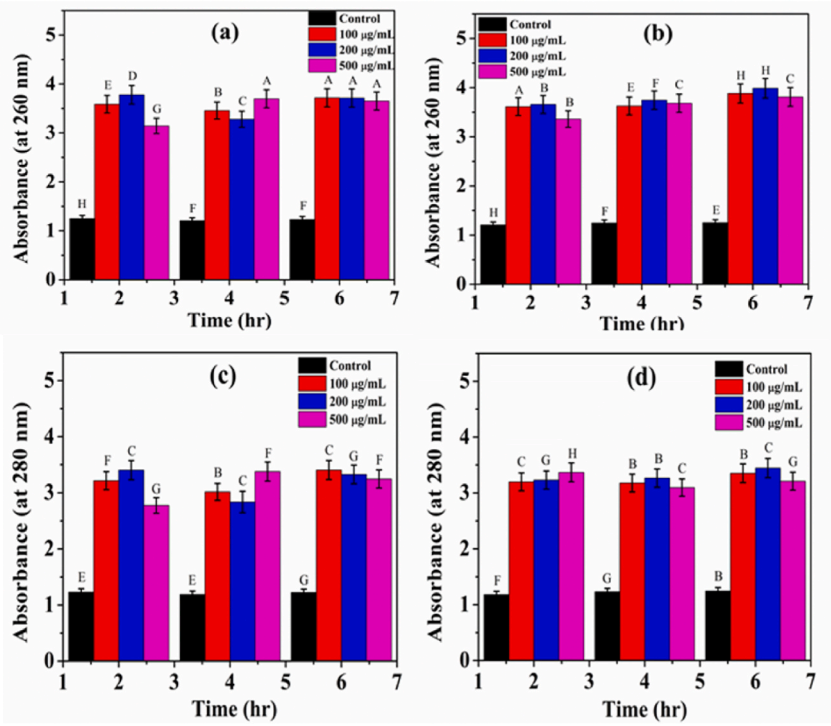

Fig. 5. Analysis of cytoplasmic DNA leakage (a) *E. coli* and (b) *S. epidermidis*. Analysis of cytoplasmic protein leakage (c) *E. coli* and (d) *S. epidermidis*. The data obtained from independently carried out experiments in triplicates were stated as mean ± SD. Tukey's multiple comparison test was used to evaluate the level of statistical significance amongst the test samples considering $p \leq 0.05$ as significant. The single alphabetic letters mentioned in the bar graphs showed significance of the study. Means that do not share a letter are significantly different.

5.2. Anti-biofilm activity of biosynthesized SeNPs

Primarily, the pathogenicity of bacteria can be determined by biofilm formation. The anti-biofilm activity of synthesized SeNPs against *S. epidermidis* and, *K. pneumonia* was analysed applying Congo red agar plate method. It was observed that, deficiency of SeNPs

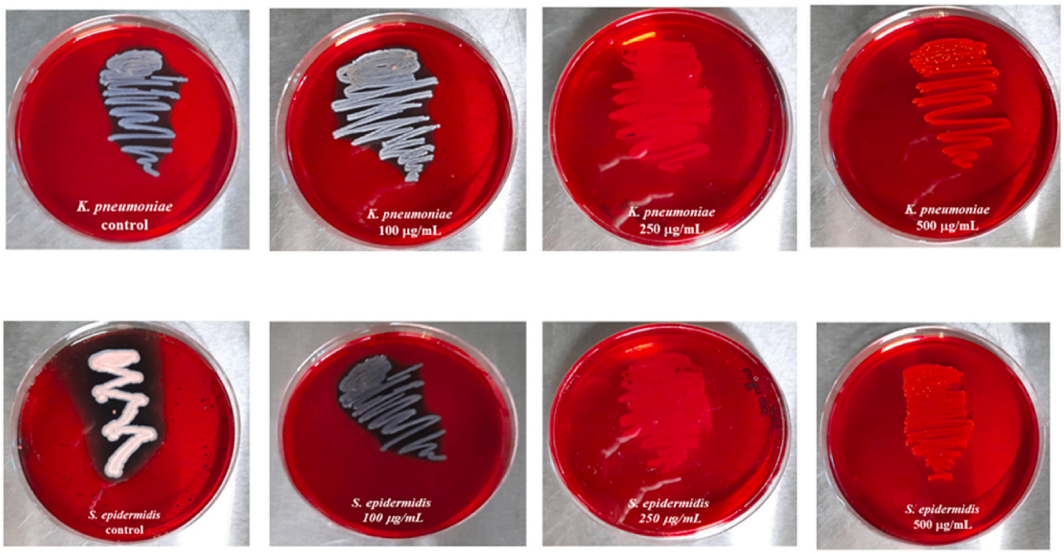

Fig. 6. Congo-red plate assay against *K. pneumoniae* and *S. epidermidis* at various concentrations of biosynthesized SeNPs to assess the anti-biofilm activity of biogenic SeNPs. (For interpretation of the references to colour in this figure legend, the reader is referred to the Web version of this article.)

results in the development of black colonies which illustrates the biofilm formation. Furthermore, the anti-biofilm activity of SeNPs was indicated by subsequent decrease of black colonies after treatment with higher concentration of SeNPs (250 and 500 μg/mL) (Fig. 6). The anti-biofilm activity of synthesized SeNPs was further confirmed using microtiter plate assay against *S. epidermidis, K. pneumonia* and *E. coli*. Additionally, the obtained anti-biofilm activity of SeNPs was compared with the anti-biofilm activity of an antibiotic such as ampicillin. As shown in Fig. 7a, with an increase in the concentration of biosynthesized SeNPs, the anti-biofilm activity against studied bacteria increased in case of *E.coli*. Additionally, for each concentration of SeNPs we have observed enhanced anti-biofilm activity in comparison to antibiotics such as ampicillin. Additionally, we have found similar results for other test organisms such as *S. epidermidis* and *K. pneumonia* (Fig. 7b & c). Hence, our results estimated the concentration-dependent antibiofilm activity of SeNPs. Notably, as reported, SeNPs have anti-biofilm activity against a wide range of bacterial strains. In this context, Cremonini et al. suggested that SeNPs might have broad spectrum anti-biofilm activity, which would make them potentially adaptable for addressing a variety of bacterial diseases [47].

6. Photocatalytic activity of biosynthesized SeNPs

The photocatalytic activity of synthesized SeNPs was evaluated via degradation of methylene blue (MB), a cationic dye under ambient condition under UV radiation. This assay has been carried out in a time dependent manner ranging from 0 to 80 min (Fig. 8). As displayed in the figure, two significant absorption peaks of MB were evidenced at 627 nm and 674 nm respectively in the UV–Vis spectra. The obtained peak at 674 nm was considered as a reference for the estimation of photocatalytic activity. As shown in the figure, upon increasing the time interval, the intensity of absorption peak for MB dye at 674 decreased, signifying the photocatalytic activity of synthesized SeNPs. This work is in good correlation with the estimation of Tripathi et al. [48].

7. Cytotoxicity assay of SeNPs

In order to gain significant idea regarding effectiveness of green synthesized SeNPs in cell death and cell survival, a cell viability assay was carried out. Fig. 9 depicted a significant relationship between various concentrations of biosynthesized SeNPs and percentage of viable cells. Here, we observed that, lower concentrations of biosynthesized SeNPs don't affect the viability of cells significantly. However, with an increase in the concentrations of SeNPs, slight reduction in cell viability was evidenced with a dose dependent manner. In this context, Afzal et al. have also validated the non-toxic nature of *Arthrospira indica* SOSA-4 mediated SeNPs, where they found the IC_{50} value to be 124 μg/mL against normal embryonic kidney cells (HEK-293) [49]. Additionally, Alam et al.

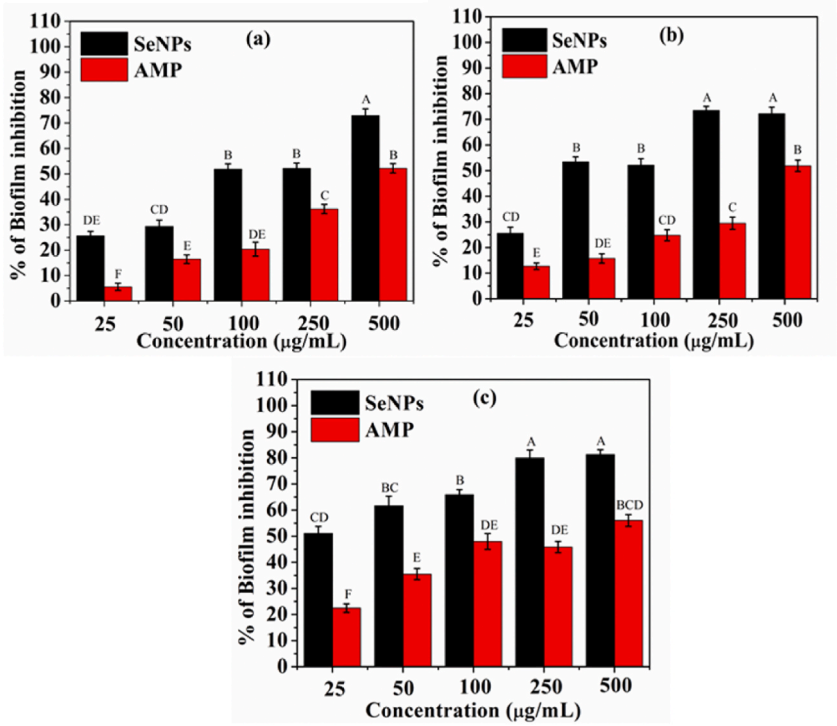

Fig. 7. Comparative analysis of anti-biofilm activity of biogenic SeNPs with ampicillin against (a) *E. coli*, (b) *S. epidermidis* and (c) *K. pneumoniae* at different concentrations of SeNPs. These experiments were carried out independently in triplicates and data were stated as mean ± SD. Tukey's multiple comparison test was used to evaluate the level of statistical significance amongst the test samples considering $p \leq 0.05$ as significant. The bar graphs indicating single alphabetic letters in the relevant study were significant. Means that do not share a letter are significantly different.

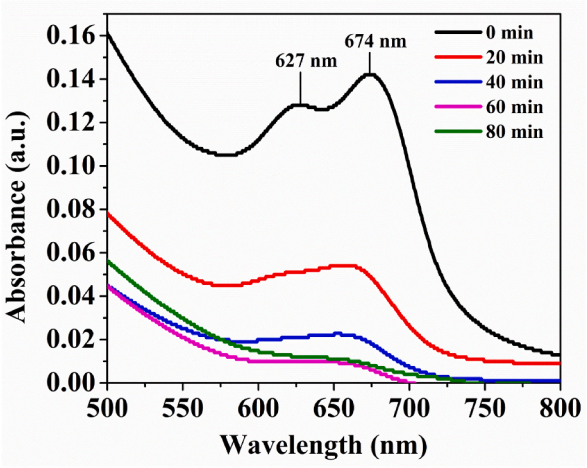

Fig. 8. Analysis of photocatalytic activity of biosynthesized SeNPs.

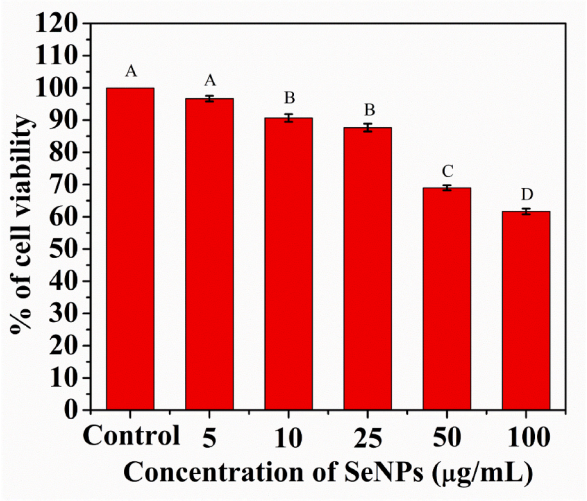

Fig. 9. Cytotoxicity assay of Synthesized SeNPs against the human embryonic kidney (HEK 293) cell line. These experiments were carried out independently in triplicates and data were reported as mean ± SD. Tukey's multiple comparison test was used to evaluate the level of statistical significance amongst the test samples considering $p \leq 0.05$ as significant. The bar graphs signifying single alphabetic letters in the respective study were significant. Means that do not share a letter are significantly different.

have also performed the cytotoxicity assay of *Psidium guanjava* mediated SeNPs against normal (CHO) cell lines and found the SeNPs to be non-toxic in nature and biocompatible towards studied cell lines [50].

8. Discussion

Recently, green synthesis of SeNPs has been widely reported from various plants, microorganisms and waste materials owing to their cost effective and ease of synthesis. Owing to the above lines, we have fabricated SeNPs from *Nyctanthes arbor-tristis* L. The present study highlights facile synthesis of SeNPs from *N. arbor-tristis* which is considered to be a mythological plant and has high medicinal advantages in Ayurveda. After the addition of leaf extract of *N. arbor-tristis* L., selenium nanoparticles were fabricated, reducing selenate into selenium, resulting in the colour change. *N. arbor-tristis* L., contains a broad range of phytochemicals including anti-oxidants as well as reducing agents like mannitol, vitamin C, carotene, flavanol glycosides, triterpenoid etc, which might be acting as reducing agents in fabrication of SeNPs [29,32]. Green synthesis using plant extracts have various advantageous effects such as safe, stable, eco-friendly and cost-effective approaches. Additionally, nanoparticles synthesized in this methods possess significant physico-chemical properties, since they might be rich in various effective phytochemical constituents [51,52]. The changed colour of the mixture was prompted by the surface plasmon resonance property of nanoparticles indicating that elemental selenium nano-particles were formed. Among, various nanoparticles, SeNPs have already appealed significant interest of different research groups for

various biological and pharmaceutical applications. Owing to their cutting-edge physico-chemical properties such as high chemical stability and electron transfer capability SeNPs are becoming a promising candidate for an extensive range of applications [33]. The SPR characteristics of SeNPs was validated by UV–visible spectroscopic analysis (Fig. 1a). UV–Visspectra displayed the broad peak at 279 nm which confirmed the fabrication of SeNPs. Additionally, in our study we found band gap energy of 4.68 eV as shown in Fig. 1b which is higher than reported in various studies ranging from 2.0 to 3.1 eV [38,53]. This study implies that, bigger the particle size, lower is the band gap energy and smaller the particle size, higher is the band gap energy [53]. FTIR analysis confirmed various bonds present in green synthesized SeNPs (Fig. 1c). Significant absorption peaks were observed which are in good agreement with Cittrarasu et al. and Kannan et al. [36,54]. Such functional groups are accountable for the synthesis and stability of synthesized SeNPs [55]. Additionally, DLS was used for hydrodynamic size analysis of synthesized SeNPs as shown in Fig. 1d. As per the data provided by DLS, size of SeNPs was slightly larger than the actual size. DLS generally measures the hydrodynamic volume of nanoparticles in the colloidal solution. It has been reported that, nanoparticles sometimes form aggregates within the colloidal solution. Therefore, DLS measures the size of the aggregates rather than the size of single nanoparticles [56,57]. Hence the size difference of nanoparticles was observed. In this context, Sharma et al. have also stated regarding the size of SeNPs synthesized from dried *Vitis vinifera* (raisin) extract [56]. The stability of colloidal solution of synthesized SeNPs was determined by zeta potential. The corresponding zeta potential of −18.4 mV was observed as shown in Fig. 2a. The X-Ray diffraction analysis revealed the crystalline structure of synthesized SeNPs (Fig. 2b). Other literatures proclaimed similar results regarding the crystallinity of SeNPs [58]. The biomolecules present in the leaf extract are liable to stabilize the shape and size of the SeNPs by providing steric hindrance or electrostatic repulsion [59]. The morphological characteristics of synthesized SeNPs was confirmed by FE-SEM analysis indicating spherical shape of SeNPs and the size of the SeNPs ranges from 60 to 80 nm (Fig. 2d). The synthesized SeNPs possess spherical morphology due to the presence of capping agents in the leaf extract. Such capping agents are essential for controlling the growth of SeNPs, resulting in spherical morphology [60]. The antioxidant property of SeNPs was confirmed by DPPH and hydrogen peroxide scavenging assay which showed that, at higher methanolic concentrations, SeNPs exhibited significant antioxidant activity and demonstrated significant scavenging activity at 250 and 500 μg/mL (Fig. 3). Lobo et al. suggested that antioxidants are compounds that can neutralize or mitigate the damaging effects of free radicals, such as H_2O_2 radicals [43]. In this regard, Alagesan et al. have demonstrated similar scavenging activity for bio-synthesized SeNPs and ascorbic acid against DPPH [38]. However, some reported studies proclaimed that, amorphous SeNPs possess excellent antioxidant activity [61]. Although, various mechanisms behind the antimicrobial efficacy of SeNPs have already been well established, however, the detailed mechanism has not yet been thoroughly investigated. Therefore, a precise and effective mechanism is crucial for safe utilization of biosynthesized SeNPs as an innovative antimicrobial agent. In this experiment, we have evaluated the antimicrobial, anti-biofilm, anti-oxidant, and photocatalytic activity of biogenic SeNPs using various biophysical and antimicrobial techniques. We have also explored the effect of SeNPs on cytoplasmic membrane integrity of bacteria as it is an essential aspect to evaluate their antibacterial mechanism. As observed from growth kinetics, SeNPs exhibited the reduction of cell viability in accordance with augmentation of the concentration of SeNPs. In this regard, San Keskin et al., and Salem et al. have also observed significant antimicrobial activity of SeNPs [44,45]. From the findings of this study, it was suggested that, biogenic SeNPs are effective in combatting both Gram-positive and Gram-negative bacteria. In relation to our findings, Salem et al. also have demonstrated a strong antibacterial activity of SeNPs at higher concentrations against an array of Gram-negative and Gram-positive bacteria [45]. Similarly, in this context, Sahoo et al. have proposed significant antibacterial activity against various bacterial strains which also revealed the concentration dependent nature of biosynthesized SeNPs [33]. Additionally, our study has also estimated a significant growth inhibition at higher concentration of SeNPs against *A. baumannii*, *E. coli* and *M. luteus* as shown in Fig. 4. The evaluation of leakage of cytoplasmic components such as nucleic acids and proteins of *E. coli* and *S. epidermidis* confirmed that biogenic SeNPs interface puts stress on bacterial membrane resulting in leakage of cytoplasmic contents as shown in Fig. 5. This is in agreement with the study conducted by Yuan et al., that SeNPs induce the rupture of bacterial cell membranes resulting in the reduction of cell viability and growth inhibition [62]. This study also assessed the anti-biofilm activity of biogenic SeNPs over *E. coli, S. epidermidis* and, *K. pneumonia* and our results estimated the concentration-dependent anti-biofilm activity of SeNPs (Figs. 6 and 7). Notably, as reported, SeNPs have anti-biofilm activity against wide range of bacterial strains. In this context, Cremonini et al. suggested that SeNPs might have broad spectrum anti-biofilm activity, which would make them potentially adaptable for addressing variety of bacterial diseases [47]. In relation to this, Shakibaie et al. have demonstrated similar results indicating strong anti-biofilm activity of biogenic SeNPs against clinical isolates of *S. aureus*, *P. aeruginosa* and *P. mirabilis* synthesized from *Bacillus* sp. MSh-1 [63]. Again, Bagheri et al. investigated antibacterial and anti-biofilm activity of SeNPs against *Vibrio cholerae* and suggested strong anti-biofilm activity at higher concentration of SeNPs [64]. However, further research is required to gain an in-depth idea regarding the mechanisms of the biofilm-inhibitory activity for biogenic SeNPs and additional selenium compounds. The experiment further assessed the photocatalytic activity of biogenic SeNPs via degradation of methylene blue (MB), a cationic dye under ambient condition with UV radiation. Two significant absorption peaks of MB were evidenced at 627 nm and 674 nm respectively in the UV–Vis spectra. The obtained peak intensity at 674 nm was further decreased with gradual increase in time indicating the estimation of photocatalytic activity. The colour of MB is due to their absorption of light in the visible spectrum 350–700 nm. Being a heterocyclic aromatic chemical compound, at para position in the central ring, MB demonstrates conjugative aromatic structure of three hexagonal rings owing to $n \rightarrow \pi^*$ transition in the structure, MB exhibits a strong blue colour. Such transition also indicated a prominent band at 674 nm in the UV spectrum. Owing to the electronic transition of the conjugative aromatic structure, another band was obtained at 627 nm [48]. Additionally, various chromophores like nitro, azo, anthraquinone moiety, phthalocyanine, methine group and auxochromes like COOH, SO_3H or OH groups are responsible for influencing the solubility of MB dye. However, the dissociation of structural bonds of the dye affects the groups like chromophore and auxochromes from the molecular structure indicating decolourization of MB dye [65]. In our study, owing to the electron relay effect, SeNPs act as an acceptor as well as a donor of electrons for MB, hence SeNPs are a catalyst for

oxidation-reduction reaction [48,66]. The reduction in central ring of MB indicates the elimination of n→π* electronic transition and its conjugative structure which subsequently leading with the formation of colourless MB and time-dependent shift of absorption peaks. This work is in good correlation with the estimation of Tripathi et al. [48]. Additionally, MTT assay was employed for evaluation of cytotoxicity of the synthesized SeNPs which signifies the cell viability based on the redox potential of cell [67]. It showed that, lower concentrations of biogenic SeNPs don't put any significant effect on viability of normal cells whereas upon increasing the concentration of biosynthesized SeNPs minimum reduction in cell viability was observed, indicating effective biocompatibility of SeNPs to perform wide range of applications. In this context, Anu et al. have performed a comparative study on cytotoxicity of chemically synthesized and biosynthesized SeNPs employing *Allium sativum* on Vero cells which revealed less toxicity of green synthesized SeNPs as compared to chemically synthesized SeNPs [68]. As well, Forootanfar et al. have also carried out a comparative study on cytotoxic effect of biosynthesized SeNPs and selenium dioxide from marine bacterial isolate *Bacillus* sp. MSh-1 and reported lower cytotoxicity in MCF-7 cells associated with selenium dioxide [69]. Additionally, as reported by Afzal et al. *Arthrospira indica* SOSA-4 mediated SeNPs were found to be non-toxic towards normal cell lines [49]. Similarly, Alam et al. have also performed the cytotoxicity assay of *Psidium guanjava* mediated SeNPs and found the non-toxic effect of SeNPs towards normal (CHO) cell lines [50]. Such studies are significant for establishment of effective biocompatibility of SeNPs towards studied cell lines. Furthermore, owing to the extensive scope of its genome project and the abundance of data acquired through developmental and genomic research, *Danio rerio* (zebrafish) appears to be a potential candidate having comprehensive applications as well as an in vivo model vertebrate for cytotoxicity evaluation [70]. Furthermore, size, husbandry and early morphogenesis of *D. rerio* make it as an excellent model for effective toxicological studies compared to other vertebrates. Therefore, *D. rerio* often used as in vivo embryonic as well as larval model in order to investigate the progressive toxicity of pollutants, microbial toxins, different nanomaterials, plastics, heavy metals and various other potentially toxic compounds [71]. Vundela et al. have investigated cytotoxic effect SeNPs on the development of *D. rerio* embryos. Various embryonic developmental defects were also investigated at subsequent time intervals with different hours-post fertilization (hpf). At 24 hpf, lower doses of SeNPs did not show any harmful effects on embryogenesis. Upon increase in hpf, SeNPs showed pericardial edema, but there was no indication of mortality. As well, higher dosage of SeNPs such as 75 and 100 μg/mL indicated hyperemia as well as pericardial edema. However, at 72 hpf, SeNPs revealed high intensities of deformities like spinal curvature, pericardial edema, as well as yolk sac edema and also higher dosage of SeNPs like 75 and 100 μg/mL exhibited no evidence of embryonic death. However, toxic effects of SeNPs on embryogenesis were evidenced at 96 hpf and death of embryo was also evidenced at 75 and 100 μg/mL of SeNPs. So they found that, SeNPs were non-toxic at lower concentration [70]. So, combining all these estimations, lower doses of SeNPs does not show any toxic effect or any death of *D. rerio* embryo indicating that, lower concentration of SeNPs shows effective biocompatibility towards *D. rerio* embryo.

9. Conclusion

The present study is crucial to validate the outcomes and to gain a comprehensive knowledge regarding potential applications of the biosynthesized SeNPs in terms of antibacterial, antibiofilm, antioxidant and photocatalytic applications. The significance of our study not only confined to specific biomedical applications, but also spans over numerous industrial and environmental applications. This study is significant since it reveals the comprehensive insight regarding the antibacterial potential of SeNPs and provides idea regarding the concentration dependent activity. These findings could serve in various fields including medicine and public health as well as industrial sectors enabling solutions to bacterial infections and related challenges. However, such analysis contributes a significant knowledge regarding the mode of action of SeNPs. Further in vivo studies are essential to establish the safety and utility of these synthesized SeNPs.

Ethical approval

Not applicable.

Funding

This research did not receive any specific grant from funding agencies in the public, commercial or not-for-profit sectors.

Data availability

All data described in this study are contained within the main article.

CRediT authorship contribution statement

Siddharth Satpathy: Writing – original draft, Validation, Methodology, Investigation, Formal analysis, Data curation, Conceptualization. **Lipsa Leena Panigrahi:** Writing – review & editing, Validation, Methodology, Investigation, Formal analysis, Data curation, Conceptualization. **Pallavi Samal:** Writing – review & editing, Data curation. **Kirti Kanta Sahoo:** Data curation. **Manoranjan Arakha:** Writing – review & editing, Validation, Supervision, Investigation, Conceptualization.

Declaration of competing interest

The authors declare the following financial interests/personal relationships which may be considered as potential competing interestsManoranjan Arakha reports a relationship with Siksha O Anusandhan that includes:If there are other authors, they declare that they have no known competing financial interests or personal relationships that could have appeared to influence the work reported in this paper.

Acknowledgments

SOA-DBT Builder National Laboratory and Department of Biotechnology, Government of India, are duly acknowledged for the support provided for DLS analysis under the DBT-Builder project with sanctioned order no BT/INF/22/SP45078/2022.

References

[1] A.F. Read, R.J. Woods, Antibiotic resistance management, Evolution, medicine, and public health 2014 (1) (2014) 147.
[2] F. Prestinaci, P. Pezzotti, A. Pantosti, Antimicrobial resistance: a global multifaceted phenomenon, Pathog. Glob. Health 109 (7) (2015) 309–318.
[3] P. Shrestha, et al., Enumerating the economic cost of antimicrobial resistance per antibiotic consumed to inform the evaluation of interventions affecting their use, Antimicrob. Resist. Infect. Control 7 (2018) 1–9.
[4] L.L. Panigrahi, B. Sahoo, M. Arakha, Nanotheranostics and its role in diagnosis, treatment and prevention of COVID-19, Front. Mater. Sci. 16 (2) (2022) 220611.
[5] L.L. Panigrahi, et al., Adsorption of antimicrobial peptide onto chitosan-coated iron oxide nanoparticles fosters oxidative stress triggering bacterial cell death, RSC advances 13 (36) (2023) 25497–25507.
[6] A. Gupta, et al., Combatting antibiotic-resistant bacteria using nanomaterials, Chem. Soc. Rev. 48 (2) (2019) 415–427.
[7] B. Sahoo, et al., Polyethylene glycol functionalized zinc oxide nanoparticle with excellent photocatalytic performance and oxidative stress mediated bacterial cell death, Opt. Mater. 148 (2024) 114891.
[8] B. Sahoo, et al., Photocatalytic activity of biosynthesized silver nanoparticle fosters oxidative stress at nanoparticle interface resulting in antimicrobial and cytotoxic activities, Environ. Toxicol. 38 (7) (2023) 1577–1588.
[9] M.K. Rai, et al., Silver nanoparticles: the powerful nanoweapon against multidrug-resistant bacteria, J. Appl. Microbiol. 112 (5) (2012) 841–852.
[10] M. Premanathan, et al., Selective toxicity of ZnO nanoparticles toward Gram-positive bacteria and cancer cells by apoptosis through lipid peroxidation, Nanomed. Nanotechnol. Biol. Med. 7 (2) (2011) 184–192.
[11] J. Ma, et al., Enhanced inactivation of bacteria with silver-modified mesoporous TiO2 under weak ultraviolet irradiation, Microporous Mesoporous Mater. 144 (1–3) (2011) 97–104.
[12] S. Shamaila, et al., Advancements in nanoparticle fabrication by hazard free eco-friendly green routes, Appl. Mater. Today 5 (2016) 150–199.
[13] N.P. Shetti, et al., Nanostructured titanium oxide hybrids-based electrochemical biosensors for healthcare applications, Colloids Surf. B Biointerfaces 178 (2019) 385–394.
[14] V. Makarov, et al., "Green" nanotechnologies: synthesis of metal nanoparticles using plants, Acta Naturae (англоязычная версия) 6 (1) (2014) 35–44, 20.
[15] M.P. Rayman, The importance of selenium to human health, The lancet 356 (9225) (2000) 233–241.
[16] A. Abdelouas, et al., Using cytochrome c 3 to make selenium nanowires, Chem. Mater. 12 (6) (2000) 1510–1512.
[17] V. Nayak, et al., Potentialities of selenium nanoparticles in biomedical science, New J. Chem. 45 (6) (2021) 2849–2878.
[18] A. Khurana, et al., Therapeutic applications of selenium nanoparticles, Biomed. Pharmacother. 111 (2019) 802–812.
[19] A. Ullah, et al., Biogenic selenium nanoparticles and their anticancer effects pertaining to probiotic bacteria—a Review, Antioxidants 11 (10) (2022) 1916.
[20] Z. Bao, et al., Method and mechanism of chromium removal from soil: a systematic review, Environ. Sci. Pollut. Control Ser. 29 (24) (2022) 35501–35517.
[21] H.-A.A. Hussein, O.M. Darwesh, B. Mekki, Environmentally friendly nano-selenium to improve antioxidant system and growth of groundnut cultivars under sandy soil conditions, Biocatal. Agric. Biotechnol. 18 (2019) 101080.
[22] J. Cui, et al., Selenium reduces cadmium uptake into rice suspension cells by regulating the expression of lignin synthesis and cadmium-related genes, Sci. Total Environ. 644 (2018) 602–610.
[23] T. Zhang, et al., Recent research progress on the synthesis and biological effects of selenium nanoparticles, Front. Nutr. 10 (2023) 1183487.
[24] B. Ao, et al., A review on synthesis and antibacterial potential of bio-selenium nanoparticles in the food industry, Front. Microbiol. 14 (2023).
[25] A.H. Hashem, S.S. Salem, Green and ecofriendly biosynthesis of selenium nanoparticles using Urtica dioica (stinging nettle) leaf extract: antimicrobial and anticancer activity, Biotechnol. J. 17 (2) (2022) 2100432.
[26] S. Pandey, et al., Biogenic synthesis and characterization of selenium nanoparticles and their applications with special reference to antibacterial, antioxidant, anticancer and photocatalytic activity, Bioproc. Biosyst. Eng. 44 (2021) 2679–2696.
[27] E. Saied, et al., Aspergillus terreus-mediated selenium nanoparticles and their antimicrobial and photocatalytic activities, Crystals 13 (3) (2023) 450.
[28] D. Indhira, et al., Antimicrobial and photocatalytic activities of selenium nanoparticles synthesized from elaeagnus indica leaf extract, Processes 11 (4) (2023) 1107.
[29] J. Agrawal, A. Pal, Nyctanthes arbor-tristis Linn—a critical ethnopharmacological review, J. Ethnopharmacol. 146 (3) (2013) 645–658.
[30] N.S. Chauhan, Medicinal and Aromatic Plants of Himachal Pradesh, Indus publishing, 1999.
[31] A. Banerjee, et al., Nyctanthes arbor-tristis Linn.–Spectrum of its bioactivity potential, Planta Med. 73 (9) (2007). SL_006.
[32] S.P. Patil, S.T. Kumbhar, K.G. Sahu, An overview on use of Nyctanthes arbor-tristis in green synthesis of nanoparticles, Nanotechnology for Environmental Engineering (2023) 1–9.
[33] B. Sahoo, et al., Oxidative stress generated due to photocatalytic activity of biosynthesized selenium nanoparticles triggers cytoplasmic leakage leading to bacterial cell death, RSC advances 13 (17) (2023) 11406–11414.
[34] M. Arakha, et al., Zinc oxide nanoparticle energy band gap reduction triggers the oxidative stress resulting into autophagy-mediated apoptotic cell death, Free Radic. Biol. Med. 110 (2017) 42–53.
[35] E. Petryayeva, U.J. Krull, Localized surface plasmon resonance: nanostructures, bioassays and biosensing—a review, Anal. Chim. Acta 706 (1) (2011) 8–24.
[36] V. Cittrarasu, et al., Green synthesis of selenium nanoparticles mediated from Ceropegia bulbosa Roxb extract and its cytotoxicity, antimicrobial, mosquitocidal and photocatalytic activities, Sci. Rep. 11 (1) (2021) 1032.
[37] C. Mellinas, A. Jiménez, M.d.C. Garrigós, Microwave-assisted green synthesis and antioxidant activity of selenium nanoparticles using Theobroma cacao L. bean shell extract, Molecules 24 (22) (2019) 4048.
[38] V. Alagesan, S. Venugopal, Green synthesis of selenium nanoparticle using leaves extract of withania somnifera and its biological applications and photocatalytic activities, Bionanoscience 9 (2019) 105–116.
[39] J.A. Hernández-Díaz, et al., Antibacterial activity of biosynthesized selenium nanoparticles using extracts of Calendula officinalis against potentially clinical bacterial strains, Molecules 26 (19) (2021) 5929.
[40] F. Yang, et al., Surface decoration by Spirulina polysaccharide enhances the cellular uptake and anticancer efficacy of selenium nanoparticles, Int. J. Nanomed. (2012) 835–844.
[41] C.P. Shah, et al., Vinyl monomers-induced synthesis of polyvinyl alcohol-stabilized selenium nanoparticles, Mater. Res. Bull. 45 (1) (2010) 56–62.

[42] N. Srivastava, M. Mukhopadhyay, Biosynthesis and structural characterization of selenium nanoparticles mediated by Zooglea ramigera, Powder Technol. 244 (2013) 26–29.
[43] V. Lobo, et al., Free radicals, antioxidants and functional foods: impact on human health, Phcog. Rev. 4 (8) (2010) 118.
[44] N.O. San Keskin, O. Akbal Vural, S. Abaci, Biosynthesis of noble selenium nanoparticles from Lysinibacillus sp. NOSK for antimicrobial, antibiofilm activity, and biocompatibility, Geomicrobiol. J. 37 (10) (2020) 919–928.
[45] S.S. Salem, et al., Antibacterial, cytotoxicity and larvicidal activity of green synthesized selenium nanoparticles using Penicillium corylophilum, J. Cluster Sci. 32 (2021) 351–361.
[46] R.P. Sharma, et al., Sol–gel auto-combustion mediated cobalt ferrite nanoparticles: a potential material for antimicrobial applications, Int. Nano Lett. 9 (2019) 141–147.
[47] E. Cremonini, et al., Biogenic selenium nanoparticles: characterization, antimicrobial activity and effects on human dendritic cells and fibroblasts, Microb. Biotechnol. 9 (6) (2016) 758–771.
[48] R.M. Tripathi, et al., Biosynthesis of highly stable fluorescent selenium nanoparticles and the evaluation of their photocatalytic degradation of dye, Bionanoscience 10 (2020) 389–396.
[49] B. Afzal, et al., Biosynthesis, characterization and biomedical potential of Arthrospira indica SOSA-4 mediated SeNPs, Bioorg. Chem. 129 (2022) 106218.
[50] H. Alam, et al., Synthesis and characterization of nano selenium using plant biomolecules and their potential applications, BioNanoScience 9 (2019) 96–104.
[51] V. Aswathi, et al., Green synthesis of nanoparticles from biodegradable waste extracts and their applications: a critical review, Nanotechnology for Environmental Engineering 8 (2) (2023) 377–397.
[52] M. Thatyana, et al., Advances in phytonanotechnology: a plant-mediated green synthesis of metal nanoparticles using phyllanthus plant extracts and their antimicrobial and anticancer applications, Nanomaterials 13 (19) (2023) 2616.
[53] A.A. Jadhav, P.K. Khanna, Impact of microwave irradiation on cyclo-octeno-1, 2, 3-selenadiazole: formation of selenium nanoparticles and their polymorphs, Rsc Advances 5 (56) (2015) 44756–44763.
[54] S. Kannan, et al., Synthesis of selenium nanorods with assistance of biomolecule, Bull. Mater. Sci. 37 (2014) 1631–1635.
[55] N. Srivastava, M. Mukhopadhyay, Biosynthesis and structural characterization of selenium nanoparticles using Gliocladium roseum, J. Cluster Sci. 26 (2015) 1473–1482.
[56] G. Sharma, et al., Biomolecule-mediated synthesis of selenium nanoparticles using dried Vitis vinifera (raisin) extract, Molecules 19 (3) (2014) 2761–2770.
[57] M. Kapur, K. Soni, K. Kohli, Green synthesis of selenium nanoparticles from broccoli, characterization, application and toxicity, Adv. Tech. Biol. Med 5 (1) (2017) 2379, 1764.
[58] M. Mehta, et al., Synthesis and characterization of MgO nanocrystals using strong and weak bases, Powder Technol. 226 (2012) 213–221.
[59] A. Hosseingholian, et al., Recent advances in green synthesized nanoparticles: from production to application, Materials Today Sustainability (2023) 100500.
[60] R. Javed, et al., Role of capping agents in the application of nanoparticles in biomedicine and environmental remediation: recent trends and future prospects, J. Nanobiotechnol. 18 (2020) 1–15.
[61] Y. Li, et al., The reversal of cisplatin-induced nephrotoxicity by selenium nanoparticles functionalized with 11-mercapto-1-undecanol by inhibition of ROS-mediated apoptosis, Biomaterials 32 (34) (2011) 9068–9076.
[62] Q. Yuan, et al., Evaluation of antibacterial activity of selenium nanoparticles against food-borne pathogens, Microorganisms 11 (6) (2023) 1519.
[63] M. Shakibaie, et al., Anti-biofilm activity of biogenic selenium nanoparticles and selenium dioxide against clinical isolates of Staphylococcus aureus, Pseudomonas aeruginosa, and Proteus mirabilis, J. Trace Elem. Med. Biol. 29 (2015) 235–241.
[64] S. Bagheri-Josheghani, B. Bakhshi, Investigation of the Antibacterial and Antibiofilm Activity of Selenium Nanoparticles against Vibrio cholerae as a Potent Therapeutics, Canadian Journal of Infectious Diseases and Medical Microbiology, 2022, p. 2022.
[65] V.V. Konduri, et al., Green synthesis of silver nanoparticles from Hibiscus tiliaceus L. Leaves and their applications in dye degradation, antioxidant, antimicrobial, and anticancer activities, South Afr. J. Bot. 168 (2024) 476–487.
[66] S.-T. Huang, et al., Synthesis, characterization, photocatalytic activity of visible-light-responsive photocatalysts BiOxCly/BiOmBrn by controlled hydrothermal method, J. Mol. Catal. Chem. 391 (2014) 105–120.
[67] L. Gunti, R.S. Dass, N.K. Kalagatur, Phytofabrication of selenium nanoparticles from Emblica officinalis fruit extract and exploring its biopotential applications: antioxidant, antimicrobial, and biocompatibility, Front. Microbiol. 10 (2019) 451408.
[68] K. Anu, et al., Green-synthesis of selenium nanoparticles using garlic cloves (Allium sativum): biophysical characterization and cytotoxicity on vero cells, J. Cluster Sci. 28 (2017) 551–563.
[69] H. Forootanfar, et al., Antioxidant and cytotoxic effect of biologically synthesized selenium nanoparticles in comparison to selenium dioxide, J. Trace Elem. Med. Biol. 28 (1) (2014) 75–79.
[70] S.R. Vundela, et al., Multi-biofunctional properties of phytofabricated selenium nanoparticles from Carica papaya fruit extract: antioxidant, antimicrobial, antimycotoxin, anticancer, and biocompatibility, Front. Microbiol. 12 (2022) 769891.
[71] A.J. Hill, et al., Zebrafish as a model vertebrate for investigating chemical toxicity, Toxicol. Sci. 86 (1) (2005) 6–19.